Response of Temperature and Density Profiles to Heat Deposition Profile and Its Impact on Global Scaling in LHD

H.Yamada 1), S.Murakami 1), K.Yamazaki 1), O.Kaneko 1), J.Miyazawa 1), R.Sakamoto 1), K.Y.Watanabe 1), K.Narihara 1), K.Tanaka 1), S.Sakakibara 1), M.Osakabe 1), B.J.Peterson 1), S.Morita 1), K.Ida 1), S.Inagaki 1), S.Masuzaki 1), T.Morisaki 1), G.Rewoldt 2), H.Sugama 1), N.Nakajima 1), W.A.Cooper 3), T.Akiyama 4), N.Ashikawa 1), M.Emoto 1), H.Funaba 1), P.Goncharov 5), M.Goto 1), H.Idei 1), K.Ikeda 1), M.Isobe 1), K.Kawahata 1), H.Kawazome 6), K.Khlopenkov 1), T.Kobuchi 1), A.Komori 1), A.Kostrioukov 1), S.Kubo 1), R.Kumazawa 1), Y.Liang 1), T.Minami 1), S.Muto 1), T.Mutoh 1), Y.Nagayama 1), Y.Nakamura 1), H.Nakanishi 1), Y.Narushima 1), K.Nishimura 1), N.Noda 1), T.Notake 7), H.Nozato 8), S.Ohdachi 1), N.Ohyabu 1), Y.Oka 1), T.Ozaki 1), A.Sagara 1), T.Saida 5), K.Saito 1), M.Sasao 1), K.Sato 1), M.Sato 1), T.Seki 1), T.Shimozuma 1), M.Shoji 1), H.Suzuki 1), Y.Takeiri 1), N.Takeuchi 7), N.Tamura 1), K.Toi 1), T.Tokuzawa 1), Y.Torii 7), K.Tsumori 1), T.Watanabe 1), T.Watari 1), Y.Xu 1), I.Yamada 1), S.Yamamoto 7), T.Yamamoto 7), M.Yokoyama 1), Y.Yoshimura 1), M.Yoshinuma 1), T.Mito 1), K.Itoh 1), K.Ohkubo 1), I.Ohtake 1), T.Satow 1), S.Sudo 1), T.Uda 1), K.Matsuoka 1), O.Motojima 1)

1) National Institute for Fusion Science, Toki, Gifu 509-5292, Japan
2) Princeton Plasma Physics Laboratory, Princeton, NJ 08544, USA
3) Centre de Recherches en Physique des Plasmas, Ecole Polytechnique Federale de Lausanne, PPB 1015, Lausanne, Switzerland
4) Research Laboratory for Nuclear Reactors, Tokyo Institute of Technology, Tokyo 152-8550, Japan
5) Department of Fusion Science, School of Mathematical and Physical Science, Graduate University for Advanced Studies, Hayama 240-0193, Japan
6) Graduate School of Energy Science, Kyoto University, Uji 611-0011, Japan
7) Department of Energy Engineering and Science, Nagoya University, Nagoya 464-8603, Japan
8) Graduate School of Frontier Sciences, The University of Tokyo, Tokyo 113-0033, Japan

e-mail contact of main author: hyamada@lhd.nifs.ac.jp

Abstract. Energy confinement and heat transport of net current-free NBI-heated plasmas in the Large Helical Device (LHD) are discussed with an emphasis on density dependence. Although the apparent density dependence of the energy confinement time has been demonstrated in a wide parameter range in LHD, the loss of this dependence has been observed in the high density regime under the specific condition. Broad heat deposition due to off-axis alignment and shallow penetration of neutral beams degrades the global energy confinement while the local heat transport maintains a clear temperature dependence lying between Bohm and gyro-Bohm characteristics. The central heat deposition inclines towards an intrinsic density dependence like $\tau_E \propto (\overline{n}_e / P)^{0.6}$ from the saturated state. The broadening of the temperature profile due to the broad heat deposition profile contrasts with the invariant property which has observed widely as profile consistency and stiffness in tokamak experiments.

1. Introduction

Studies on the energy confinement and heat transport of net current free plasmas have progressed due to the recent experiments in Large Helical Device (LHD) [1] with upgraded heating capability up to 9 MW of NBI. The NBI lines are arranged in the tangential direction and the energy of the NBI ranges between 120-150 keV in this study. The apparent density dependence of the energy confinement time as described in the ISS95 scaling [2] has been demonstrated [3,4] in the extended wide parameter regimes in LHD. This favorable density dependence observed in LHD is of importance from the prospect of net current-free plasmas

towards high confinement and high β by high density operation. When the plasma profiles are fixed, the density dependence of the energy confinement time, i.e., $\tau_E \propto (\bar{n}_e / P)^{0.6}$ or $\tau_E \propto (\bar{n}_e / P)^{0.5}$ can be interpreted by the gyro-Bohm local heat conduction as $\chi \propto T^{3/2}$ or the Bohm as $\chi \propto T$, respectively. Since the density dependence of the global confinement and the temperature dependence of the local heat transport are two sides of the same physical mechanism, it is also attracting interest to the physics issue of anomalous transport.

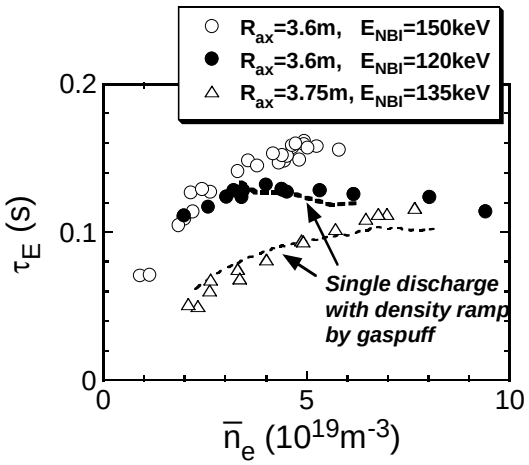

Fig.1 Dependence of energy confinement time on density. Closed circles: R_{ax}=3.6m, P_{NBI}=4.7MW, E_{NBI}=120keV. Open circles: R_{ax}=3.6m, P_{NBI}=4.3MW, E_{NBI}=150keV. Open triangles: R_{ax}=3.75m, P_{NBI}=4.1MW, E_{NBI}=135keV. Dotted lines:traces of the single discharges with density ramp-up.

Although the existence of this kind of density dependence has been verified in many toroidal experiments, its absence also has been reported [5]. Recent experiments employing a wide range of heating power in LHD have indicated that the favorable density dependence saturates at a certain density under specific conditions. This paper discusses the cause of this saturation and the related characteristics of anomalous transport. Through this study, the response of the temperature profile to the heat deposition profile is highlighted, which contrasts with the concept of stiffness or profile consistency observed in many tokamaks.

2. Experimental Results

Confinement improvement by shifting the magnetic axis inward already has been demonstrated in LHD [3]. Saturation of the energy confinement time with the increase in density has been observed in gas-fueled NBI-heated plasmas, particularly, in this inward shifted configuration with R_{ax}=3.6 m. Closed circles in Fig.1 shows the data in the density flat phase for a series of density scans with a fixed heating power of 4.7MW and the averaged beam energy E_{NBI} of 120 keV in the case with R_{ax}=3.6m and B = 2.8 T. The energy confinement time ceases to increase above 4×10^{19}m^{-3}. This density regime is one third of the empirical density limit [6]. Indeed this saturated state can be maintained in a quasi-steady state and extended close to 1×10^{20}m^{-3} by this heating power. The increase of the beam energy mitigates this saturation. The density scan with E_{NBI} of 150 keV raises this performance density

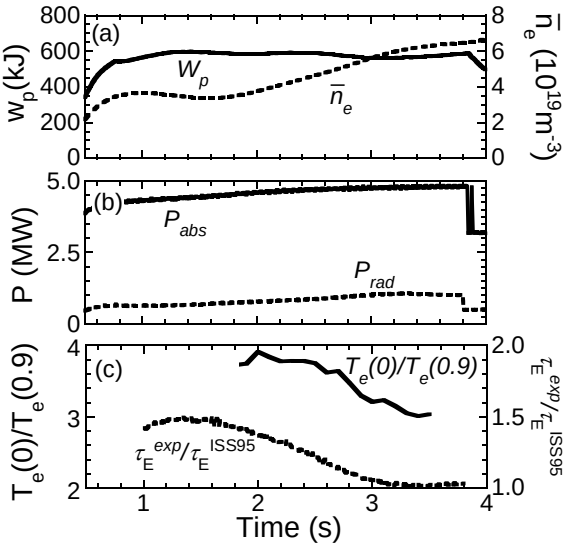

Fig.2 Waveforms of the discharge with density ramp-up in the case with R_{ax}=3.6m, P_{NBI}=4.7MW, E_{NBI}=120keV. (a) Stored energy and line averaged density. (b) Absorbed power of NBI and total radiation power. (c) Ratio of the central electron temperature to that at ρ=0.9 and improvement factor of energy confinement time on ISS95.

limit to 5×10^{19}m^{-3}(see open circles in Fig.1). Although the heating power in the scan with E_{NBI} of 150 keV is 10 % less than that with E_{NBI} of 120 keV, the deterioration of confinement in the case with E_{NBI} of 120 keV can not be attributed to simple power degradation. The other case with R_{ax}=3.75m and B = 2.64 T shows a contrasting result (see triangles in Fig.1). Although the absolute value of the energy confinement time is worse than in the case with R_{ax}=3.6m [3], the density dependence is maintained close to the operational density limit.

The saturation or degradation of confinement is highlighted in the density ramp-up phase by gas-puffing in a single discharge with R_{ax}=3.6 m. The discharge shown in Fig.2 corresponds to the thick dotted line in Fig.1. The line averaged density is doubled from t = 1.5 s to 4.0 s, however, the stored energy and the energy confinement time do not change. The improvement factor on ISS95 is degraded from 1.5 to 1. The ratio of the radiation power to the absorbed power increases from 16 % to 22 % which is well below the condition of radiation collapse. The radiation is also localized at the plasma edge. Therefore the radiation loss does not play an essential role in confinement saturation. Although temperatures decrease with the increase in density, the decrease of electron temperature is more distinguished in the center than in the edge. The degradation of confinement seems to coincide with a broadening of temperature profile.

The discharge in the case with R_{ax}=3.75m indicates a contrasting behavior to the case with R_{ax}=3.6m. The temporal behavior shown in Fig. 3 corresponds to the thin dotted line in Fig.1. The stored energy increases monotonically with the increase in density. The confinement degradation referred to ISS95 and broadening of temperature profile in the high density region is much mitigated compared to the case with R_{ax}=3.6m. A slight difference in the condition of the NBI does not explain this distinguished result.

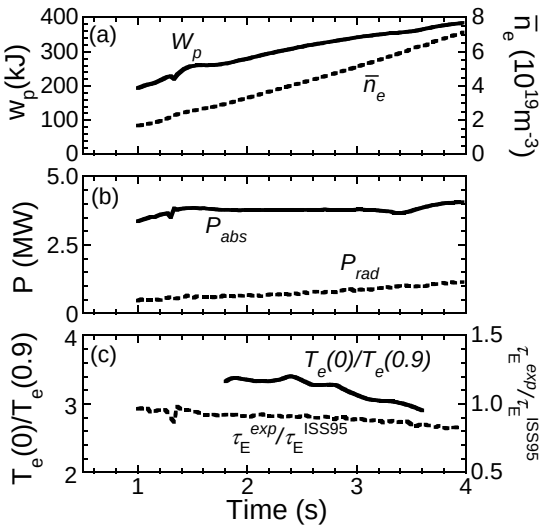

Fig.3 Waveforms of the discharge with density ramp-up in the case with R_{ax}=3.75m, P_{NBI}=4.1MW, E_{NBI}=135keV..(a) Stored energy and line averaged density. (b) Absorbed power of NBI and total radiation power. (c) Ratio of the central electron temperatures to that at ρ=0.9 and improvement factor of energy confinement time on ISS95.

The temporal changes of the density and temperature profiles, and the power balance are investigated for two discharges with R_{ax}=3.6m and R_{ax}=3.75m illustrated in Fig.2 and 3, respectively. Figure 4 shows the case with R_{ax}=3.6m. The density profile remains flat during the density ramp-up and the electron temperature becomes broad with the increase in density. The high density operation prevents the deep penetration of tangentially injected neutral beams and heat deposition moves from the core to the periphery (see Fig.4(c)). This tendency is emphasized with the inward-shifted magnetic axis due to the off-axis heating because of the tangency radius of 3.7 m of the NBI beam lines and the broad density profile due to gas-puffing particularly in the density ramp-up phase. Broadening of the temperature profile correlates with broadening of the power deposition profile. The local heat transport is investigated for time slices in the density ramp-up phase. Although the density dependence going as $\tau_E \propto \bar{n}_e^{0.6}$ is lost completely, the local heat conduction coefficient shows a temperature dependence with the

power between 1.1 and 1.6 at both radii of ρ=0.5 and 0.9 (see Fig.4(d)). The transport of NBI heated plasmas has no significant dependence on collisionality [4], which suggests that the thermal conductivity does not depend on density. The density dependence in the energy confinement time is derived from the replacement of the temperature dependence by the heating power and density. The clear dependence of the thermal conductivity on the temperature shown in Fig.4(d) supports this argument. The discussion of whether the transport is Bohm or gyro-Bohm requires clarification of the dependence on the magnetic field strength, however, the essential point is that the apparent contradiction between the global confinement and the local transport can be qualitatively explained by the change of the heat deposition profile.

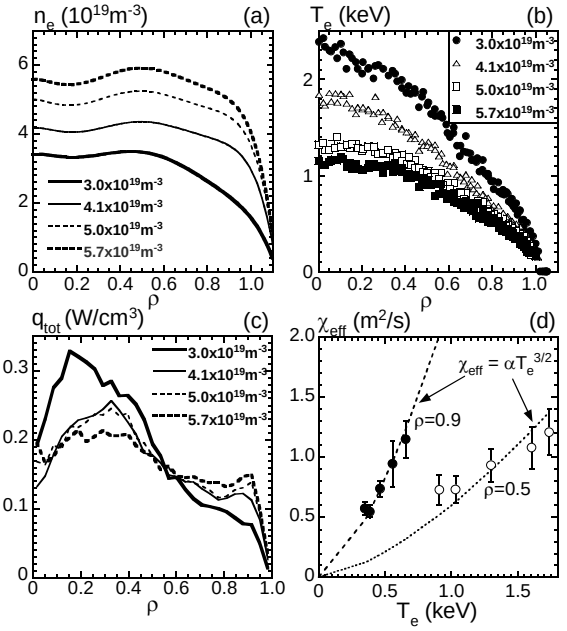

Fig.4 Plasma profiles at different times in the discharge (#28168) shown in Fig.2. (a) Density. (b) Temperature. (c) Power deposition. (d) Temperature dependence of thermal diffusivity at two radii of ρ=0.5 (open circles) and ρ=0.9 (solid circles) derived from the power balance analysis of 5 time slices.

In contrast to the case with R_{ax}=3.6m, the degradation of the energy confinement time due to the density ramp-up is mitigated in the case with R_{ax}=3.75m. Since the geometrical arrangement of tangential NBI's is optimized for the central heating in this configuration, the heat deposition profile is peaked and insensitive to the increase in density (see Fig.5(a)) in this case. The thermal diffusivity shows a clear temperature dependence as in the case with R_{ax}=3.6m, which is consistent with the behavior of the energy confinement time because of the unchanged heat deposition profile.

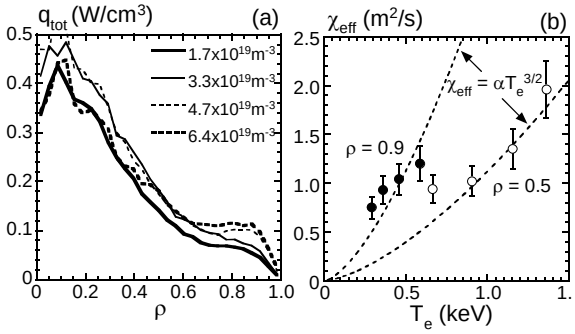

Fig.5 (a) Profile of power deposition from NBI in the discharges in the case with R_{ax}=3.75m. (b) Temperature dependence of thermal diffusivity at two radii of ρ=0.5 (open circles) and ρ=0.9 (solid circles) derived from the power balance.

The above discussion on the correlation between the power deposition profile and the global energy confinement time reminds a simple picture where the central heating is favorable for the global confinement. The advantage of the higher beam energy is related to this argument. Two data points with different beam energy in Fig.1 are compared in Fig.6. These two plasmas have almost the same heating and absorbed power, and line-averaged density but different beam energies. The energy confinement is 25 % better in the higher beam energy case than in the lower beam energy case, which cannot be explained by the heating power dependence. The case with E_{NBI} of 150 keV indicates the peaked power deposition profile due to deep penetration and higher central electron temperature in spite of 10 % less total power. Here the linkage between the central heating deposition and the global energy confinement

through no invariant in the electron temperature is observed.

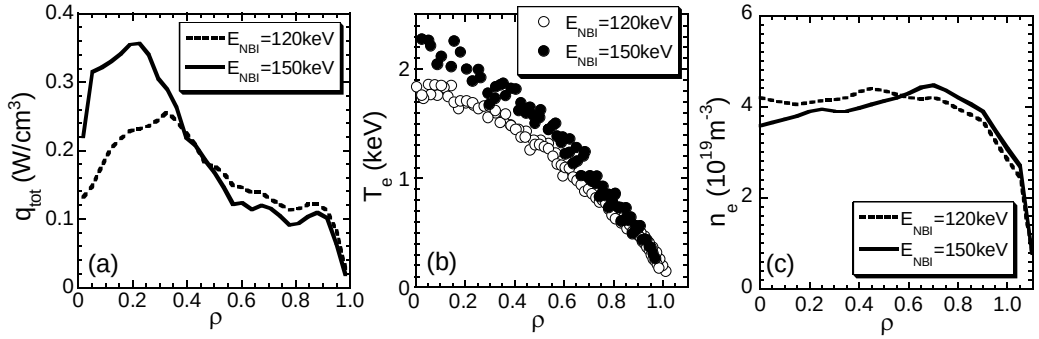

Fig.6 Plasma profiles in discharges with different NBI conditions. (a) Heat deposition. (b) Electron temperature. (c) Electron density. Dotted lines and open circles:P_{NBI}=4.7MW, E_{NBI}=120keV (#28168). Solid lines and closed circles: P_{NBI}=4.3MW, E_{NBI}=150keV (#28936).

3. Discussions and Conclusions

A major part of an apparent contradiction between the global energy confinement time and local thermal diffusivity, which has been observed in the case with R_{ax}=3.6m, can be explained by the broadening of heat deposition. These observations are linked with the fact that the temperature profile changes straight-forwardly according to the heat deposition profile of the net current free plasmas in LHD. The experimental results described in this paper are added to examples that net-current free plasmas do not have a clear invariant like concepts of stiffness and profile consistency in tokamaks [7]. The apparent discrepancy between the global and the local transport suggests that the central heating improves the saturated state and indeed this effect is demonstrated by the increased beam energy.

It should be noted that the difference in the power deposition profile alone does not explain the change of density dependence of the energy confinement time completely. It is probable that the response of the magnetic island [8] and some confinement improvement related to the central heating contribute to these phenomena.

The favorable density dependence can be extended towards much higher density by pellet fueling [9] in both cases of R_{ax}=3.6 m and 3.75 m. The peaked density profile realized by pellet fueling promotes the core heating and recovers the intrinsic density dependence when the density is moderate. However, the peripheral heat deposition becomes predominant even in the peaked density profile by pellet injection above 8×10^{19}m^{-3}, therefore, another mechanism related to confinement improvement is prerequisite to explain the advantage of pellet injection.

Acknowledgements

The authors acknowledge the continuous efforts of all members of the device engineering group to reliably operate LHD.

Reference

[1] MOTOJIMA, O., et al., OV/1-6 in this conference.
[2] STROTH, U., et al., Nucl. Fusion **36** (1996) 1063.
[3] YAMADA, H., et al., Nucl. Fusion **41** (2001) 901.
[4] YAMADA, H., et al., Plasma Phys. Control. Fusion **43** (2001) A55.
[5] STROTH, U., Plasma Phys. Control. Fusion **40** (1998) 9.
[6] SUDO, S., et al., Nucl. Fusion **30** (1990) 11.
[7] WAGNER, F., et al., Phys. Rev. Lett. **56** (1986) 2187.
[8] OHYABU, N., et al., Phys. Rev. Lett. **88** (2002) 055005-1.
[9] SAKAMOTO, R., et al., Nucl. Fusion **41** (2001) 381.